A MODEL FOR NANOSIZE SILICON PARTICLE FORMATION IN A THERMAL PLASMA EXPANSION REACTOR

B. Micheel*, D. Hansen, N. Rao, S. Girshick, J. Heberlein and P. McMurry

University of Minnesota, 111 Church St. S. E., Minneapolis, MN 55455.
* Currently at Trinity Consultants, Inc., Overland Park, KS 66210.

ABSTRACT

A numerical model for nanoparticle formation and growth in a plasma expansion reactor is presented. The nanosized particles are generated by injecting reactants into a plasma downstream of a DC arc, and quenching the reacting mixture in a subsonic nozzle expansion. Nucleation and growth of particles in the nozzle is modeled using a discrete-sectional aerosol dynamics model coupled to a one-dimensional nozzle flow model. Particle growth by coagulation downstream of the nozzle is modeled assuming a locally self preserving particle size distribution. The modeling results are in qualitative agreement with experimental measurements.

1. INTRODUCTION

Materials obtained by consolidating nanosize powders have generated considerable interest due to their remarkable mechanical, electrical, optical and magnetic properties [1]. Thermal plasma processes provide an attractive route for the high-rate production of fine powders [2], especially those of high temperature ceramics. We have recently used a thermal plasma expansion process [3,4] to synthesize silicon, carbon and silicon carbide nanoparticles with narrow size distributions. The particles are generated by injecting gas phase reactants ($SiCl_4$ and/or CH_4) into an Ar or Ar-H_2 plasma downstream of a DC arc, and quenching the hot gases by subsonic expansion through a ceramic-lined converging nozzle. The "hot-wall" converging nozzle design used here minimizes boundary layer effects, thus favoring the formation of particles with uniform properties in the nozzle. Once formed, however, these particles may further grow by coagulation, and may eventually form agglomerates in the cooling flow far downstream of the nozzle. We have previously reported results from calorimetric measurement of plasma conditions [3] and measurement of particle properties using aerosol techniques [3,4] for our process. This paper is a continuation of previous work and presents a numerical model for particle formation and growth in the plasma reactor for the case of silicon synthesis. The model is useful in interpreting experimental data and also provides guidance for further refinement and optimization of the process.

The plasma expansion reactor system being modeled is described elsewhere in these proceedings [5] and consists of a DC arc torch downstream of which is a 75 mm

long ceramic flow channel. The upper part of this channel is a cylindrical ring (i.d. 15 mm) provided with holes for radial injection of reactants. The lower portion of the channel is a converging nozzle with a length L of 50 mm and exit diameter d_n of 5 mm. The nozzle discharges into a large diagnostics chamber maintained at 400 torr by a self scrubbing pump. Particles in the aerosol jet exiting the nozzle are extracted by an ejector-dilutor probe having a capillary inlet (length=9 cm, i.d.=0.16 cm). The aerosol sample is diluted downstream of the capillary to freeze its size distribution before being characterized by an aerosol mobility size spectrometer [4]. Representative size distributions obtained with this instrument for Si and SiC were similar, being lognormal in both cases, with a number mean diameter ~ 10 nm and a geometric standard deviation ~ 1.6. As has been noted in our earlier work, the similarity of the distributions for Si and SiC particles suggests a common origin, and it is believed that the SiC particles are formed by the nucleation of small Si particles followed by carburization in a hydrocarbon rich atmosphere. In that case, the nucleation model for silicon also provides a starting point for modeling SiC particle formation in our system.

We present below a two-part model for particle formation and growth in our plasma system. In section 2, the evolution of silicon particle size distributions in the nozzle is calculated using a discrete-sectional aerosol dynamics model [6,7] coupled to a one-dimensional nozzle flow [8]. In section 3, the growth of particles downstream of the nozzle is predicted using a non-isothermal coagulation model [9] coupled to empirical models for the jet and sampling probe flow. Concluding remarks are made in section 4.

2. MODEL FOR PARTICLE FORMATION IN THE NOZZLE

The nucleation and growth of silicon particles in the nozzle has been calculated assuming a one-dimensional compressible flow corrected for area change, wall friction, and heat transfer to nozzle walls [8]. The starting point of the nucleation calculation is the nozzle entrance, where the relatively slow moving gases are assumed to have reached chemical equilibrium. For typical conditions at the nozzle entrance (temperature T ~ 3000 K, pressure P ~ 0.67 atm), equilibrium calculations show that $SiCl_4$ disocciation to form Si vapor is virtually complete. As the flow accelerates through the nozzle the temperature drops rapidly, but the short residence times (~ 0.1 ms) ensure that the silicon chemistry is essentially frozen in the nozzle. The high cooling rate (~ 5×10^6 K/s) in the nozzle expansion causes the silicon vapor to become highly supersaturated, thus providing a driving force for homogeneous nucleation.

The clustering and evaporation of silicon atoms to nucleate particles is modeled using a discrete-sectional aerosol dynamics code [6,7] which solves population balance equations for the entire particle size range of interest, i.e. from monomers, dimers, trimers, etc. to large stable particles. For computational efficiency, separate equations are written only for the smaller discrete sizes, while the larger sizes are grouped into size sections, typically spaced logarithmically by particle volume.

The population balance equations for monomers in the non-isothermal nozzle flow may be written as

$$\frac{D\hat{n}_1}{Dt} = \frac{R}{\rho_g} - \rho_g \hat{n}_1 \sum_{j=1}^{\infty} \beta_{1,j} \hat{n}_j + \sum_{j=2}^{\infty} \left(1+\delta_{2,j}\right) E_j \hat{n}_j, \qquad (1)$$

while for dimers and all larger j-mers (clusters containing j monomers) the balance equations take the form,

$$\frac{D\hat{n}_k}{Dt} = \frac{1}{2}\rho_g \sum_{i+j=k} \beta_{ij}\hat{n}_i\hat{n}_j - \rho_g \hat{n}_k \sum_{i+j=k} \beta_{jk}\hat{n}_j + E_{k+1}\hat{n}_{k+1} - E_k\hat{n}_k, \quad k \geq 2. \quad (2)$$

In these equations $\hat{n}_j$ denotes the number of j-mers per unit mass of gas, R is the monomer generation or depletion rate by gas-phase chemical reactions (which under the frozen chemistry assumption equals zero), β_{ij} is the collision-frequency function for collisions between i-mers and j-mers, E_j is the evaporation coefficient for j-mers, and the Kronecker delta function δ_{2j} accounts for the fact that two monomers are created by evaporation from a dimer. The functions β and E are obtained from gas kinetic theory and thermodynamic considerations, respectively [3].

For modeling silicon nucleation in the nozzle, we have simultaneously solved a total of 50 population balance equations, including separate equations for clusters up to size 30, and for 20 sections respresenting larger clusters. These equations were fully coupled to the flow equations through the gas temperature, velocity and density. A typical calculation required about 20 CPU secs on a Cray-2 supercomputer.

Numerical results for our actual nozzle geometry and for conditions corresponding roughly to experimental data are given in Figs. 1 and 2. Fig. 1 is a plot showing the variation of the normalized silicon monomer concentration C and of the vapor saturation ratio S along the length of the nozzle. The saturation ratio is seen to rise steeply, peaking at a value S ~ 33 at a nozzle location corresponding to x/L ~ 0.6, where x is the distance from the inlet and L is the nozzle length. Within a short distance downstream of this peak, almost all the vapor condenses to growing clusters, this rapid change signifying a nucleation burst having a duration of ~ 30 μs. Note that the high cooling rate causes S to rise again at the nozzle exit, but the effect of a second nucleation burst is negligible due to vapor depletion.

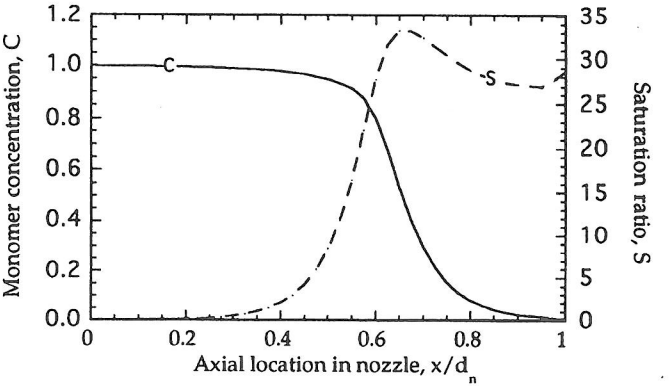

Fig. 1. Predicted silicon monomer conentration C, and saturation ratio S as a function of axial position in nozzle.

The discrete-sectional approach is also capable of providing detailed information on the evolving particle size distribution, including subcritical clusters and down to the

monomer. Fig. 2 shows the calculated particle size distributions at several different nozzle locations. The onset of nucleation is seen in the rapid increase in the number of larger clusters for x/L > 0.6. At the nozzle exit (x/L=1), the particles already have a

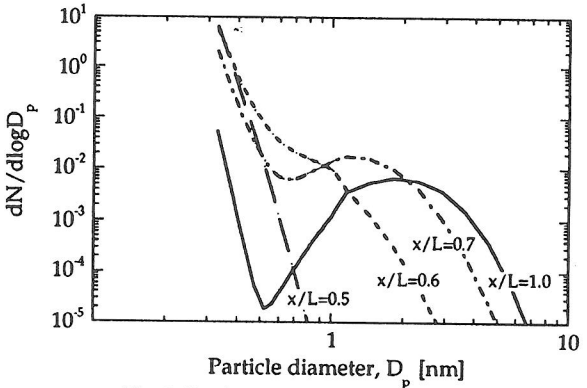

Fig. 2. Evolution of calculated particle size distribution in nozzle for silicon.

distribution with a shape similar to that observed experimentally for Si and SiC. The predicted average size of particles leaving the nozzle is around 2 nm, considerably smaller than the average size measured experimentally (~ 10 nm). Note, however, that the experimental measurements were obtained using a probe at sampling locations downstream of the nozzle exit. It is thus necessary for our theory to account for particle growth by coagulation in the nozzle jet and in the sampling capillary before a comparison with experiment can be made. This is the focus of the next section.

3. MODELING PARTICLE COAGULATION GROWTH

The particle laden flow leaving the nozzle forms an aerosol jet as it discharges into the diagnostics chamber. The aerosol dynamics in the jet is controlled by particle coagulation and mixing/entrainment, both of which tend to reduce the particle concentration (we assume that further nucleation and condensation is negligible due to vapor depletion). Coagulation in the capillary probe may also be significant for small sampling flow rates (i.e. high residence times). Aerosol coagulation in the non-isothermal, presumably turbulent nozzle jet and in the sampling capillary can be modeled using the self preserving size distribution approach of Friedlander and coworkers [9]. The coagulation model is coupled to simple flow models for the nozzle jet [10], and the sampling capillary.

Experimental data for silicon indicate that the particle size distributions measured at various axial locations in the jet have similar shapes. Assuming that the aerosol distribution is locally self preserving, the particle number concentration along the jet axis may be written as

$$\frac{dN_m}{dX} = -\frac{1}{U}\left[\frac{\alpha}{2}\left(\frac{6k_BT}{\rho_p}\right)^{1/2}\left(\frac{3}{4\pi}\right)^{1/6}\rho_g V_m^{1/6} N_m^{1/6}\right] - \frac{N_m}{X}, \qquad (3)$$

where N_m is the total particle number concentration per unit mass of gas, V_m is the aerosol volume concentration per unit mass of gas, X is the axial distance from the nozzle exit, U is the axial velocity, T is the temperature, ρ_g is the gas density, and α=6.67. The two terms in the right hand side of Eq. (3) represent respectively, the decrease in N_m due to coagulation, and due to mixing/entrainment. U and T along the jet axis are assumed to decay hyperbolically according to an empirical flow model [10], which is valid in the region $X/d_n>4$. A linear interpolation is used in the region $0 < X/d_n < 4$. In the sampling capillary, T is taken to be constant at the inlet value, and U is obtained from room temperature calibration with theoretical corrections to account for local temperature at the sampling location.

Equation (3) is solved numerically using intial conditions at the nozzle exit supplied by the nozzle model in section 2. Two limiting cases are considered for the variation of aerosol volume concentration along the jet axis: (i) V_m is assumed constant, i.e. there is no mixing; and (ii) V_m is assumed to decay hyperbolically due to mixing. Results from these calculations are shown in Fig. 3, which is a plot of the average particle diameter D_p as a function of the sampling location X downstream of the nozzle. The dashed and dotted lines represent respectively, the predicted particle diameters at the sampling location for cases (i) and (ii). It is seen here that the decay rate of V_m along the jet axis has a significant effect on the diameter growth rate, with the removal of aerosol from the axis tending to retard the growth rate. Actual experimental conditions are expected to lie between the two limiting cases, and closer to case (i). For this case, the effect of coagulation in the capillary is also shown in Fig. 3 as a solid line. This curve represents the final particle diameter obtained at the capillary outlet when sampling at location X. Particle coagulation in the probe is observed to be significant at sampling locations close to the nozzle exit, where the gas temperature is higher and the capillary flow rates smaller. For small X, this increased

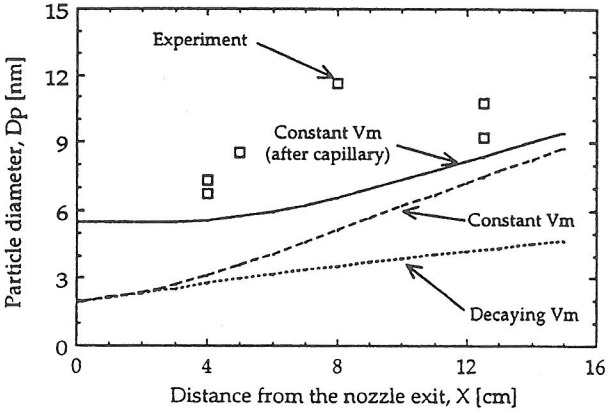

Fig. 3. Growth of particles by coagulation in the nozzle jet and sampling capillary.

coagulation has the effect of flattening out variations in D_p downstream of the capillary. Also shown in this figure are experimental data, which appear to qualitatively follow theoretical trends, though the measured particle sizes are larger than predicted. Given the many simplifications made in the model, and related uncertainties in the flow and temperature fields, the agreement is considered reasonable.

4. CONCLUSION

A numerical model for nanoparticle formation in a thermal plasma expansion reactor has been presented. The model predicts the nucleation and growth of silicon particles in the quenching nozzle, and also the diameter increase due to coagulation downstream of the nozzle and in the sampling capillary. Comparison with experimental results indicate that the model predicts experimentally observed trends qualitatively, but underpredicts particle growth rates.

ACKNOWLEDGEMENTS

This work has been supported by the National Science Foundation (NSF/ECS-9118100) and the Minnesota Supercomputer Institute.

REFERENCES

1. R. W. Siegel, *Mater. Sci. and Eng.* **A168**, 189 (1993).

2. T. Yoshida, in *Combustion and Plasma Synthesis of High-Temperature Materials*, Z.A. Munir and J.B. Holt, eds., VCH, New York, 328-339, (1990).

3. N. Rao, S. Girshick, J. Heberlein, P. McMurry, M. Bench, S. Jones, D. Hansen and B. Micheel, accepted for publication, *Plasma Chem. Plasma Proc.* (1995).

4. N. Rao, B. Micheel, D. Hansen, C. Fandrey, M. Bench, S. Girshick, J. Heberlein, and P. McMurry, accepted for publication, *J. Mater. Res.*, (1995).

5. D. Hansen, B. Micheel, N. Rao, S. Girshick, J. Heberlein, P. McMurry, *12th ISPC Proceedings*, Aug. 21-25, 1995.

6. N. Rao and P. H. McMurry, *Aerosol Sci. Technol.* **11**,120 (1989).

7. S. L. Girshick and C.-P. Chiu, *Plasma Chem. Plasma Process.* **9**, 355 (1989).

8. A. H. Shapiro and W. R. Hawthorne, *J. Appl. Mech.* **14**, A317 (1947).

9. W. Koch and S. K. Friedlander, *Part. Part. Syst. Charact.* **8**, 86 (1991).

10. P. C. Huang, W. L. T. Chen, J. V. Heberlein and E. Pfender, *10th ISPC Proceedings*, Vol. 1,1 (1991).